Solving Multi-Scale Low Frequency Electromagnetic Problems

Zhi-Guo QIAN[1], Mao-Kun LI[3], Zu-Hui MA[2], Li-Jun JIANG[2], and Weng Cho CHEW[1,2]

[1]*University of Illinois, Urbana-Champaign, IL, USA*
[2]*The University of Hong Kong, Hong Kong SAR, China*
[3]*Schlumberger-Doll Research, Cambridge, MA, USA*
Email: wcchew@hku.hk, w-chew@uiuc.edu
(WCC is on leave of absence from the University of Illinois at Urbana Champaign)

***Abstract*—In this paper, we will discuss two methods to tackle the low-frequency, multi-scale electromagnetics problem. First we will discuss the augmented electric field integral equation (AEFIE), and then, we will discuss the equivalence principle algorithm (EPA). The AEFIE allows the solution of such problems without the need to perform a loop search of a complex structure. The EPA allows the separation of circuit physics from wave physics in a multiscale problem. Hybridization of these two methods will be discussed.**

I. Introduction

There is a need to solve efficiently low frequency problems associated with multiscale, complex structures in electromagnetics [1]. The solutions of these problems are instrumental in the modelling of complex electronic package structures found in modern integrated circuit design, small antennas, and small sensors. Furthermore, they will find applications in the modelling of micro and nano structures in nano-technology and nano-biotechnology. The regime of low-frequency problems is where circuit physics dominates over wave physics. The physics of electromagnetic fields is quite different in this regime compared to higher frequency electromagnetic fields [2].

A popular way to solve such problems is to use integral equation methods [3]. However, integral equation methods have low frequency breakdown. This is due to that at low frequency, the electric field and the magnetic field are weakly coupled, compared to the wave-physics regime. Hence, most numerical methods designed do not capture these two physical phenomena well and hence, the breakdown.

Integral equation methods are attractive because in many situations, they require fewer unknowns to model a complex structure compared to differential equation methods. However, integral equation methods are often more difficult and complex compared to differential equation methods. Differential equation methods are simpler to work with. With recent advances in fast algorithms for integral equation methods, they can outperform differential equation methods in speed and memory requirements.

We will also discuss the augmented electric field integral equation (A-EFIE) approach in solving the low-frequency breakdown problem as encountered in circuits in electronic packaging [4]. In this method, the EFIE is augmented with an additional charge unknown, and an additional continuity equation relating the charge to the current. The resultant equation, after proper frequency normalization, is frequency stable down to very low frequency. This method apparently does not suffer from the low-frequency breakdown, but it does have the low-frequency inaccuracy problem. We will discuss the use of the perturbation method to derive accurate solutions when the low-frequency inaccuracy problem occurs.

When the wavelength is sizeable compared to the structure, than wave physics becomes important, and it is important that a simulation method can capture the wave physics interaction. When a structure is multi-scale, and has parts that are small compared to wavelength, but at the same time, is on the order of wavelength, then both circuit physics and wave physics are important. A simulation method has to capture both physics. In this paper, we will discuss the use of the equivalence principle algorithm (EPA) [5] to capture the multi-scale physics of multiscale complex structures by breaking a large problem into a set of smaller problems. In EPA, complex structures are partitioned into parts by the use of equivalence surfaces. The interaction of electromagnetic field with structures within the equivalence surface is done through scattering operators working via the equivalence currents on the equivalence surfaces. The solution within the equivalence surface can be obtained by various numerical methods, including AEFIE. Then the interaction between equivalence surfaces is obtained via the use of translation operators. When accelerated with the mixed-form fast multipole method, large multi-scale problems can be solved in this manner.

II. Augmented Electric Field Integral Equation

Recently, we have developed a stable electric field integral equation (EFIE) using an augmentation technique [4], [6]. This method treats the charge as an unknown and introduces an additional equation to relate the current and the charge [7]. The final matrix equation has the generalized saddle point form [8]. This technique avoids the use of loop-tree decomposition, and provides a stable EFIE formulation down to very low frequencies. The search for loops and trees of a highly complex structure is often very challenging. This method, obviating that need, heralds a new way of solving low-frequency electromagnetic, complex structure, problems with multi-scale features. In this method, the electric field integral equation (EFIE) can be written in a matrix form as

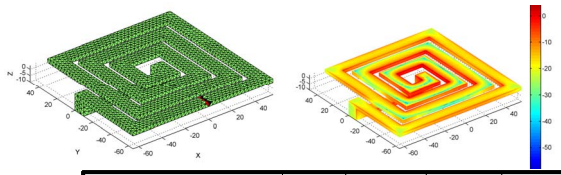

Mesh	A	B	C	D
Number of unknowns	9894	39576	158304	633216
Matrix filling time (s)	14.2	57.2	154	593
Number of Iterations	32	46	65	94
Iteration time (s)	2.57	24.0	146	725
Average time per iteration (s)	0.08	0.52	2.25	7.71

Figure 1. Simulation of a spiral inductor with increasing mesh density with no sign of low-frequency breakdown.

$$\left(ik_0\eta_0\bar{\mathbf{V}}+\frac{\eta_0}{ik_0}\bar{\mathbf{S}}\right)\cdot\mathbf{J}=\mathbf{b} \tag{1}$$

where

$$\begin{aligned}\left[\bar{\mathbf{V}}\right]_{m,n}&=\mu_r\int_{S_m}\boldsymbol{\Lambda}_m(\mathbf{r})\cdot\int_{S_n}g(\mathbf{r},\mathbf{r}')\boldsymbol{\Lambda}_n(\mathbf{r}')\,dS'\,dS\\ \left[\bar{\mathbf{S}}\right]_{m,n}&=\varepsilon_r^{-1}\int_{S_m}\nabla\cdot\boldsymbol{\Lambda}_m(\mathbf{r})\int_{S_n}g(\mathbf{r},\mathbf{r}')\nabla'\cdot\boldsymbol{\Lambda}_n(\mathbf{r}')\,dS'\,dS\\ \left[\bar{\mathbf{P}}\right]_{m,n}&=\varepsilon_r^{-1}\int_{T_m}h_m(\mathbf{r})\int_{T_n}g(\mathbf{r},\mathbf{r}')h_n(\mathbf{r}')\,dS'\,dS\end{aligned} \tag{2}$$

In the above, $\boldsymbol{\Lambda}_i(\mathbf{r})$ is the RWG basis function [9]. The scalar potential matrix $\bar{\mathbf{S}}$ can be factorized as

$$\bar{\mathbf{S}}=\bar{\mathbf{D}}^T\cdot\bar{\mathbf{P}}\cdot\bar{\mathbf{D}} \tag{3}$$

where $\bar{\mathbf{D}}$ has the meaning of a divergence operator. The current continuity condition yields

$$\bar{\mathbf{D}}\cdot\mathbf{J}=ik_0c_0\boldsymbol{\rho} \tag{4}$$

where c_0 is the speed of light.

Combining (6), (3), and (4), we get the A-EFIE as

$$\begin{bmatrix}\bar{\mathbf{V}} & \bar{\mathbf{D}}^T\cdot\bar{\mathbf{P}}\\ \bar{\mathbf{D}} & k_0^2\bar{\mathbf{I}}\end{bmatrix}\cdot\begin{bmatrix}ik_0\mathbf{J}\\ c_0\boldsymbol{\rho}\end{bmatrix}=\begin{bmatrix}\eta_0^{-1}\mathbf{b}\\ \mathbf{0}\end{bmatrix} \tag{5}$$

where $\bar{\mathbf{I}}\in\mathbb{R}^{p\times p}$ is an identity matrix, and $\boldsymbol{\rho}\in\mathbb{C}^{p\times 1}$ is the vector of charge coefficient. The matrix has a 2×2 block structure. More details about this work can be found in reference [6].

In Figure 3, we show the simulation of a spiral inductor with increasing mesh density going from Mesh A to Mesh D. The inductor value was calculated correctly at 0.62 nH but with no sign of low-frequency breakdown as the mesh density is increased. Low frequency breakdown is usually accompanied by non-convergence of iterative methods.

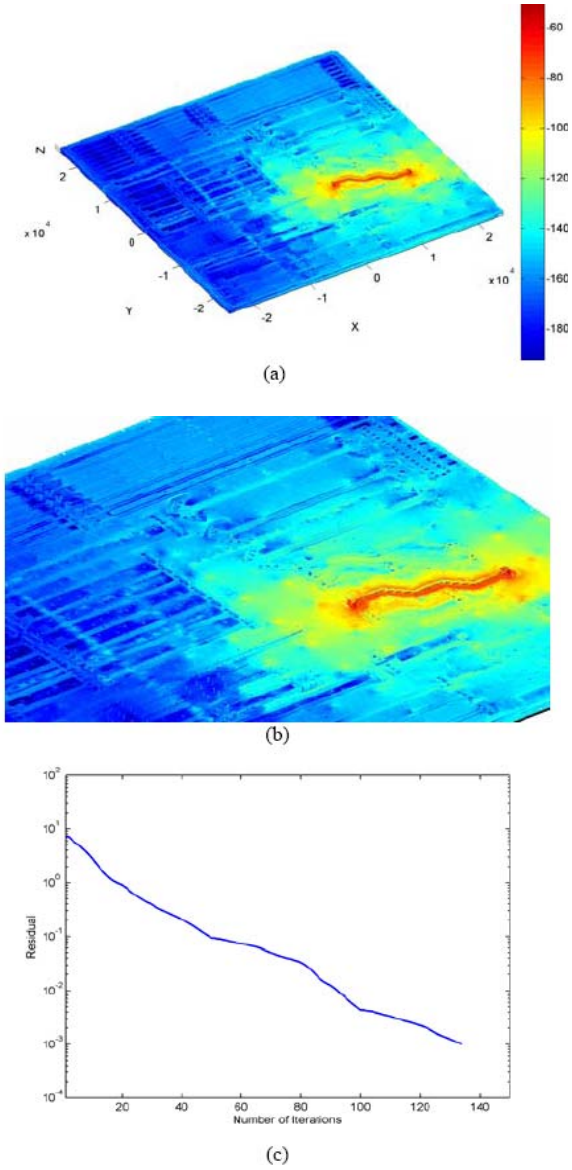

Figure 2. A full package simulation. There are four layers and 222 nets. (a) Surface electric current distribution on the full package is in dB scale. Unit: A/m. The discretization has 1 007 691 inner edges. Geometry unit: μm . (b) The close-up of the current is around the excitation. (c) The iteration history is shown. GMRES reduces the residual error to 1.E-3 with 134 iterations.

The result of simulating a full package, real world problem with over 1 million unknowns is shown in Figure 4. The problem can be solved with 134 iterations in about 1.5 hours on a 3 GHz, Dell, single CPU machine. Constraint preconditioner was used in the iterative method using GMRES. The code is accelerated with the mixed-form fast multipole algorithm [10].

III. Pertubation Method

AEFIE does suffer from the low-frequency problem, but it can be remedied with a perturbation method without the need to search for the loop of the complex structures. To this end, we expand the matrices and vectors in (5) into a perturbation series. For instance, the following matrix can be expanded as:

$$\overline{\mathbf{V}} = \overline{\mathbf{V}}^{(0)} + \delta\overline{\mathbf{V}}^{(1)} + \delta^2\overline{\mathbf{V}}^{(2)} + O\left(\delta^3\right) \tag{6}$$

We do the same to the other matrices to arrive at the perturbation equations. Then, by low frequency analysis, we obtain a series of perturbation equations from which the unknown currents and charges can be solved accurately without the low-frequency inaccuracy problem. Figure 3 shows the use of the perturbation method to arrive at a capacitance calculation without losing accuracy at low frequencies [11].

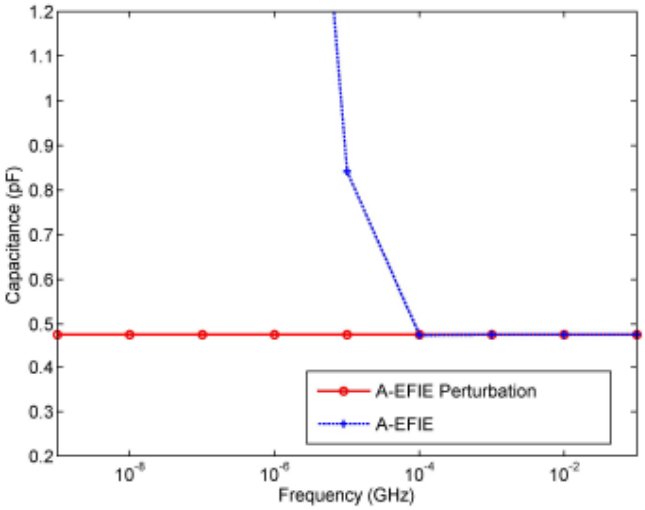

Figure 3. Comparison of the extracted capacitance between A-EFIE and A-EFIE with perturbation.

IV. Equivalence Principle Algorithm

The equivalence principle algorithm (EPA) is a good way to domain-decompose a larger problem into smaller problems. It also allows regions of low frequency physics (circuit physics) to be separated from the regions of mid frequency physics (wave physics). The use of EPA allows a larger problem to be broken down into a sum of smaller problems, so that only smaller problems need to be solved at one time. Then the solution to the larger problem is accomplished by rigorously concatenating the smaller problems together.

Recently, we have developed an equivalence principle algorithm that allows the equivalence surface to cut through metal, and break an object involving metal into smaller objects [5][12] (Figure 4). EPA also allows one to use one technique to solve the smaller problems, and a different technique for the larger problem. This is important since the physics at the micro-scale is quite different from the physics at the macro-scale.

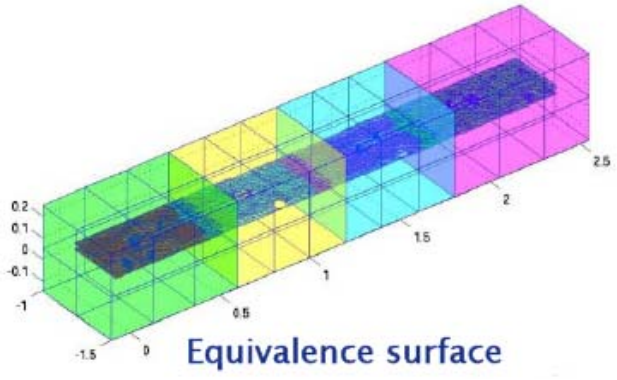

Figure 4. Equivalence surfaces are used to break a large object into smaller objects to facilitate easier solutions.

$$\mathcal{S} = \underbrace{\begin{bmatrix} -\hat{\mathbf{n}}' \times \mathcal{K} \\ -\frac{1}{\eta}\hat{\mathbf{n}}' \times \mathcal{L} \end{bmatrix}}_{\text{inside-out}} \cdot \underbrace{[\mathcal{L}_{pp}]^{-1}}_{\text{current-solver}} \cdot \underbrace{\begin{bmatrix} -\mathcal{L} & -\eta\mathcal{K} \end{bmatrix}}_{\text{outside-in}} \tag{7}$$

The physics of the scattering is encapsulated in the equivalence surfaces. The incident field from outside is first generated by equivalence currents on the equivalence surface (Figure 5). Then the current induced on the scatterer is found by MOM, and the scattered field is first used to generated equivalence currents on the equivalence surface. These equivalence currents can be used to find the scattered field everywhere outside. In this manner, a scattering operator can be defined.

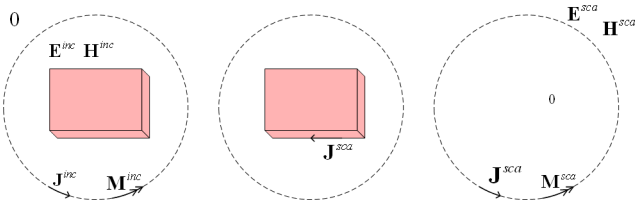

Figure 5. (Left) The incident field is propagated onto the scatterer using equivalence currents on the equivalence surface. (Middle) The current on the scatterer due to incident field is solved for using MOM. (Right) The scattered field is transmitted to infinity using equivalence currents on the equivalence surface again.

Then interactions between multiple objects need to be accounted for. They can be done using the translation operator which finds equivalence currents on one equivalence surface due to equivalence currents on another equivalence surface. The translation operator is defined as:

$$\mathcal{T}^{hh} \cdot \begin{bmatrix} \mathbf{J}_1 \\ \frac{1}{\eta}\mathbf{M}_1 \end{bmatrix} = \begin{bmatrix} -\hat{\mathbf{n}} \times \mathcal{K}^S_{HJ} & -\frac{1}{\eta}\hat{\mathbf{n}} \times \mathcal{L}^S_{HM} \\ -\frac{1}{\eta}\hat{\mathbf{n}} \times \mathcal{L}^S_{EJ} & -\hat{\mathbf{n}} \times \mathcal{K}^S_{EM} \end{bmatrix} \cdot \begin{bmatrix} \mathbf{J}_1 \\ \frac{1}{\eta}\mathbf{M}_1 \end{bmatrix} \tag{8}$$

Consequently, when multiple objects are interacting with each other, their interactions can be described by the scattering operators and translation operators defined above (Figure 6). For instance, the interaction between three objects can be described as:

$$
\begin{aligned}
\begin{bmatrix} \mathbf{J}_1^{sca} \\ \frac{1}{\eta}\mathbf{M}_1^{sca} \end{bmatrix} - \mathcal{S}_{11}\cdot\mathcal{T}_{12}^{hh}\cdot\begin{bmatrix} \mathbf{J}_2^{sac} \\ \frac{1}{\eta}\mathbf{M}_2^{sca} \end{bmatrix} - \mathcal{S}_{11}\cdot\mathcal{T}_{13}^{hp}\cdot\mathbf{J}_3 &= \mathcal{S}_{11}\cdot\begin{bmatrix} \mathbf{J}_1^{inc} \\ \frac{1}{\eta}\mathbf{M}_1^{inc} \end{bmatrix} \\
-\mathcal{S}_{22}\cdot\mathcal{T}_{21}^{hh}\cdot\begin{bmatrix} \mathbf{J}_1^{sac} \\ \frac{1}{\eta}\mathbf{M}_1^{sca} \end{bmatrix} + \begin{bmatrix} \mathbf{J}_2^{sac} \\ \frac{1}{\eta}\mathbf{M}_2^{sca} \end{bmatrix} - \mathcal{S}_{22}\cdot\mathcal{T}_{23}^{hp}\cdot\mathbf{J}_3 &= \mathcal{S}_{22}\cdot\begin{bmatrix} \mathbf{J}_2^{inc} \\ \frac{1}{\eta}\mathbf{M}_2^{inc} \end{bmatrix} \\
\mathcal{T}_{31}^{ph}\cdot\begin{bmatrix} \mathbf{J}_1^{sca} \\ \frac{1}{\eta}\mathbf{M}_1^{sca} \end{bmatrix} + \mathcal{T}_{32}^{ph}\cdot\begin{bmatrix} \mathbf{J}_2^{sca} \\ \frac{1}{\eta}\mathbf{M}_2^{sca} \end{bmatrix} + \mathcal{L}_{33}^{S}\cdot\mathbf{J}_3 &= -\mathbf{E}_3^{inc}
\end{aligned}
\tag{9}
$$

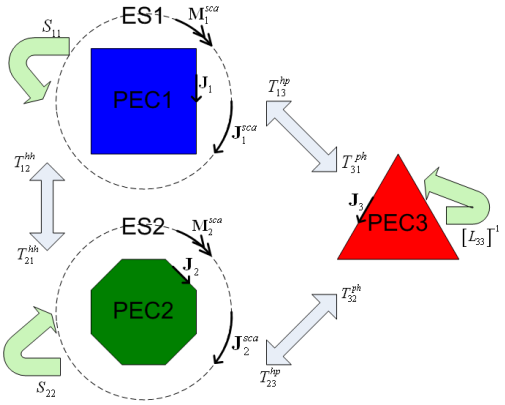

Figure 6. Multiple objects can be concatenated by using EPA.

Figure 7 shows the use of EPA to simulate the multiscale problem of an XM antenna on top of a car. The unknown count involved for EPA is 355, 305, and the code has been accelerated with 8 level MLFMA. GMRES(50) was used to reduce the residual error to 2.E-2 after 200 iterations. The total memory usage was 2.6 GB, and the computer used was a single processor Dell Precision 670, taking 54.2 s per iteration.

We can also use EPA concept to break a large 30 by 30 antenna array into tiny problems (Figure 8). The antenna array problem constitutes 7.2 million unknowns. Using EPA, the unknown count is reduced to 0.86 million (since only unknowns on equivalence surface are needed) with total memory usage of 12 GB. The problem can be solved to 2.0x10-2 precision with 149 iterations on a Dell Precision 690 with Intel XEON 3 GHz computer.

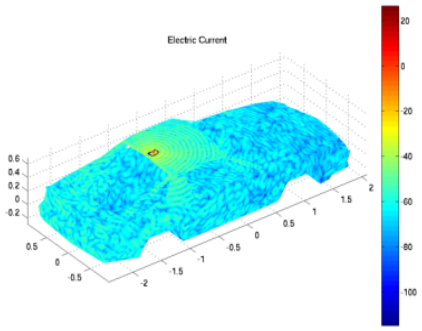

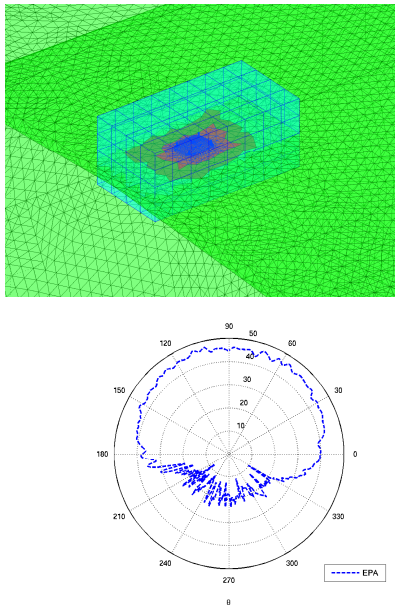

Figure 7. Multi-scale simulation of an XM antenna on a car, where the radiation pattern can be calculated.

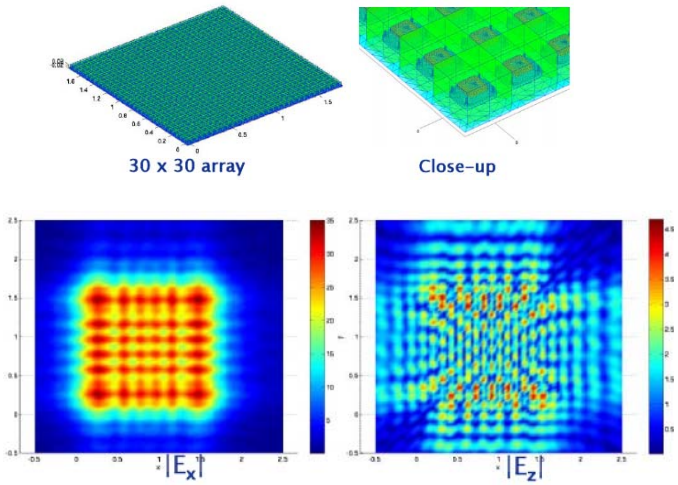

Figure 8. A large antenna array can be broken into tiny pieces using EPA allowing a large problem to be solved.

V. Conclusions

Computational electromagnetics is an interesting field. However, its future lies in its ability to perform multi-physics and multi-scale calculations in order to solve the next-generation technology problems. The rapid increases in computational speed in computers plus their memory capacity, and their miniaturization make their use increasingly pervasive. With the increasing use of computational electromagnetics, traditional pencil and paper calculations can be replaced with computer calculations. The use of simulation in engineering and science allows us to explore ideas that are previously unexplored. However, simulations do not represent reality, and point check with experiments is still

important. Also, many systems that are simulated are not realizable, and when simulating complex systems, it is also important to consider their realizability.

REFERENCES

[1] W. C. Chew, J. M. Jin, E. Michielssen, and J. M. Song, (editors), *Fast and Efficient Algorithms in Computational Electromagnetics,* Artech House, Boston, MA, 2001.

[2] W. C. Chew, "Computational Electromagnetics---the Physics of Smooth versus Oscillatory Fields," *Philo. Trans. Royal Soc. London Series A, Math., Phys. Eng. Sci.* vol. 362, no. 1816, pp. 579-602, March 15, 2004.

[3] R.F Harrington**,** Field Computation by Moment Methods, MacMillan, New York, 1968.

[4] Z. G. Qian and W. C. Chew, "A quantitative study of the low frequency breakdown of EFIE," *Microwave and Opt. Tech. Lett.,* vol. 50, no. 5, pp. 1159-1162, May 2008.

[5] M. K. Li and W. C. Chew, "A Domain Decomposition Scheme Based on Equivalence Theorem," *Micro. Opt. Tech. Lett*., v. 48, no. 9, pp. 1853-1857, Sept. 2006.

[6] Z.-G. Qian, and W.C. Chew, "Fast full-wave surface integral equation solver for multiscale structure modeling," *IEEE Transactions on Antennas and Propagation*, AP-57, no. 11, pp. 3594-3601, 2009.

[7] A. Bendali, "Numerical analysis of the exterior boundary value problem for the time-harmonic Maxwell equations by a boundary finite element method. II. The discrete problem," *Math. Comp*., vol. 43, no. 167, pp. 47-68, 1984.

[8] M. Benzi, G. H. Golub, and J. Liesen, "Numerical solution of saddle point problems," *Acta Numerica*, vol. 14, pp. 1-137, Apr. 2005.

[9] S.M. Rao, D.R. Wilton, and A.W. Glisson, Electromagnetic scattering by surfaces of arbitrary shape, *IEEE Trans Antennas Propagat* AP-30, 409-418, 1982.

[10] L.J. Jiang and W.C. Chew, "A mixed-form fast multipole algorithm," *IEEE Trans. Antennas Propag*. AP-53 (12), pp. 4145-4156, 2005**.**

[11] Z.G. Qian and W.C. Chew, "Enhanced A-EFIE with Perturbation Method," UIUC-ECE Research Report No.: CCEML 2-09, August 27, 2009.

[12] M. K. Li and W. C. Chew, "Wave-Field Interaction with Complex Structures Using Equivalence Principle Algorithm," *IEEE Trans. Antenn. Propag*., vol. 55, no. 1, pp. 130-138, 2007.